

# Cytochrome P450 2B1 Mediates Complement-dependent Sublytic Injury in a Model of Membranous Nephropathy\*

Received for publication, July 19, 2010, and in revised form, September 27, 2010. Published, JBC Papers in Press, October 14, 2010, DOI 10.1074/jbc.M110.165498

Hua Liu<sup>†1</sup>, Niu Tian<sup>†1</sup>, Istvan Arany<sup>‡</sup>, Steven A. Bigler<sup>§</sup>, David J. Waxman<sup>¶</sup>, Sudhir V. Shah<sup>||</sup>, and Radhakrishna Baliga<sup>‡2</sup>

From the Departments of <sup>†</sup>Pediatrics and <sup>§</sup>Pathology, University of Mississippi Medical Center, Jackson, Mississippi 39216, the <sup>¶</sup>Division of Cell and Molecular Biology, Department of Biology, Boston University, Boston, Massachusetts 02215, and the <sup>||</sup>Division of Nephrology, Department of Internal Medicine, University of Arkansas for Medical Sciences, Little Rock, Arkansas 72205

Membranous nephropathy is a disease that affects the filtering units of the kidney, the glomeruli, and results in proteinuria accompanied by loss of kidney function. Passive Heymann nephritis is an experimental model that mimics membranous nephropathy in humans, wherein the glomerular epithelial cell (GEC) injury induced by complement C5b-9 leads to proteinuria. We examined the role of cytochrome P450 2B1 (CYP2B1) in this complement-mediated sublytic injury. Overexpression of CYP2B1 in GECs significantly increased the formation of reactive oxygen species, cytotoxicity, and collapse of the actin cytoskeleton following treatment with anti-tubular brush-border antiserum (anti-Fx1A). In contrast, silencing of CYP2B1 markedly attenuated anti-Fx1A-induced reactive oxygen species generation and cytotoxicity with preservation of the actin cytoskeleton. Gelsolin, which maintains an organized actin cytoskeleton, was significantly decreased by complement C5b-9-mediated injury but was preserved in CYP2B1-silenced cells. In rats injected with anti-Fx1A, the cytochrome P450 inhibitor cimetidine blocked an increase in catalytic iron and ROS generation, reduced the formation of malondialdehyde adducts, maintained a normal distribution of nephrin in the glomeruli, and provided significant protection at the onset of proteinuria. Thus, GEC CYP2B1 contributes to complement C5b-9-mediated injury and plays an important role in the pathogenesis of passive Heymann nephritis.

Membranous nephropathy is a leading cause of primary nephrotic syndrome in adults (1). Despite aggressive therapy, progressive renal impairment that leads to end-stage renal disease occurs (2). Passive Heymann nephritis (PHN)<sup>3</sup> is an animal model of membranous nephropathy in which the heterologous phase is complement-dependent and neutrophil-

independent. It can be induced by a single intravenous injection of heterologous anti-tubular brush-border antiserum (anti-Fx1A), resulting in subepithelial deposits (3). Proteinuria is the hallmark of sublytic glomerular injury and is coincident with the localization of the C5b-9 membrane attack complex (MAC) early in these subepithelial deposits (4, 5).

Several pathophysiological mechanisms, including disruption and alteration of cytoskeleton proteins, have been implicated as the pathogenesis of proteinuria in membranous nephropathy (3, 6, 7). Salant *et al.* have demonstrated a complement-dependent disruption of the actin cytoskeleton, which supports the normal foot process architecture (3), as early as 1 h following exposure to anti-Fx1A and fresh human serum (8). The actin-binding protein gelsolin is a highly conserved multifunctional protein that has been localized to the podocyte (9, 10) and plays an important role in the dynamic rearrangement of the cytoskeletal architecture (11). Reactive oxygen species (ROS) and catalytic iron have been considered to be important mediators of this glomerular injury (7, 12, 13), although there is little information regarding the intracellular site for the generation of ROS and the source of iron capable of catalyzing free radical reactions.

Cytochrome P450 (CYP) is a family of heme protein monooxygenases that generate superoxide anion and hydrogen peroxide during the course of NADPH-dependent electron transfer (14, 15). The hydrogen peroxide and organic hydroperoxides can oxidatively degrade the CYP heme protein and promote the release of iron from the heme chelate (16). Recent studies, including ours, indicate that CYP plays an important role in several models of acute injury, including ischemia-reperfusion injury to the lungs and kidneys (17, 18) and acute renal failure (19, 20).

CYP2B1 has been identified in the glomerular epithelial cell (GEC) (21); however, its role in an immune-mediated glomerular disease such as PHN has not been previously examined. We postulate that CYP2B1 can serve as a source of ROS and catalytic iron and thus play an important role in alteration of the cytoskeleton, which has been implicated in the pathophysiology of proteinuria. We therefore conducted *in vitro* studies by manipulating CYP2B1 expression in the GEC and *in vivo* studies utilizing CYP inhibitors in rats.

## EXPERIMENTAL PROCEDURES

**Cell Culture**—Rat GECs (kindly provided by Dr. S. Kasi-nath, University of Texas Health Science Center) were maintained in DMEM/F-12 medium (1:1) supplemented with 10%

\* This work was supported in part by National Institutes of Health Grant 5 P42 ES07381 (to D. J. W.). This work was also supported by the Intramural Research Support Program through the University of Mississippi Medical Center (to R. B.), by American Heart Association Grant-in-aid 0655716Z (to I. A.) and by the Superfund Research Program at Boston University (to D. J. W.).

<sup>1</sup> Both authors contributed equally to the analytical data.

<sup>2</sup> To whom correspondence should be addressed: Dept. of Pediatrics, University of Mississippi Medical Center, Research Wing R116A, 2500 North State St., Jackson, MS 39216. Tel.: 601-984-5971; Fax: 601-815-5902; E-mail: rbaliga@umc.edu.

<sup>3</sup> The abbreviations used are: PHN, passive Heymann nephritis; MAC, membrane attack complex; ROS, reactive oxygen species; CYP, cytochrome P450; GEC, glomerular epithelial cell; FHS, fresh human serum; HIS, heat-inactivated human serum; LDH, lactate dehydrogenase.

## CYP2B1 in Membranous Nephropathy

fetal bovine serum, 100 units/ml insulin, and 5% penicillin/streptomycin in a humidified atmosphere of 5% CO<sub>2</sub> and 95% air at 37 °C and fed at intervals of 3 days as described (22).

**Adenovirus Infection**—GECs grown in 6-well plates were incubated in full medium containing 1 × 10<sup>8</sup> infectious units/ml adenovirus vector that contains the rat *CYP2B1* (23) for 3 h at 37 °C. The cells were then washed with culture medium and further incubated in full medium for 24 h at 37 °C. Empty adenovirus (Ad-Null, Vector BioLabs, Philadelphia, PA) was used as a negative control.

**CYP2B1 Gene Silencing**—The experiments were performed in 6-well plates (Dharmacon, Chicago, IL) in triplicate when cells reached 60–70% confluency according to the manufacturer's recommendation. In brief, the transfection reagent (DharmaFECT 1; 6 μl/well) and rat *CYP2B1* siRNA (ON-TARGETplus SMARTpool L-081876-01-0010) solution (20 nM) was prepared. These two components were mixed and added to an antibiotic-free complete medium, and the cells were incubated for 48 h in 5% CO<sub>2</sub> and 95% air at 37 °C. The extent of knockdown was determined by real-time RT-PCR and Western blotting as described (21).

**Measurement of Intracellular H<sub>2</sub>O<sub>2</sub> Generation**—The intracellular generation of H<sub>2</sub>O<sub>2</sub> in GECs was assayed using the oxidant-sensitive fluorescent dye 2',7'-dichlorodihydrofluorescein diacetate (24). In brief, when cultured GECs became confluent after adenovirus infection or gene silencing as described previously, GECs were harvested by trypsinization and suspended in Hanks' balanced salt solution. GECs were then treated with anti-Fx1A (4 mg/ml) for 40 min at 22 °C, followed by incubation with fresh human serum (FHS) or heat-inactivated human serum (HIS) (5%) at 37 °C for 1 h. The cell suspension was then transferred to a microplate (two 5 × 10<sup>5</sup> cells/well) and incubated at room temperature with dichlorodihydrofluorescein diacetate (10 μg/ml) for 30 min. At the end of the incubation, the fluorescence intensity of the cell suspension was read up to 2 h using a fluorescence plate reader (excitation at 485 nm and emission at 535 nm).

**Measurement of Cytotoxicity**—Cytotoxicity was assessed by the CytoTox-ONE™ homogenous membrane integrity assay kit (Promega, Madison, WI). Accordingly, when cultured GECs became confluent after adenovirus infection and/or gene silencing as mentioned above, GECs were treated with anti-Fx1A (4 mg/ml) for 40 min at 22 °C, followed by incubation with FHS or HIS (5%) at 37 °C for 18 h. An aliquot of the growth medium was removed and saved. The monolayer was lysed according to the manufacturer's recommendation, and lactate dehydrogenase (LDH) content was determined by a colorimetric substrate in both the medium and cell lysate. LDH release was calculated as a percentage of LDH content in the medium compared with the total LDH content (medium + lysate) (25).

**Real-time RT-PCR**—Real-time RT-PCR assays were performed using iQ™ SYBR® Green Supermix in an iCycler iQ™ real-time PCR detection system (Bio-Rad). *CYP2B1* primers were designed using the sequence obtained from rat *CYP2B1* (GenBank™ accession number J00719): forward sequence, 5'-CGCATGGAGAAGGAGAAGTC-3'; and reverse sequence, 5'-GCCGATCACCTGATCAATCT-3'. Gelsolin primer se-

quences were as follows: forward sequence, 5'-CCACT-GCGTCGCGGGG-3'; and reverse sequence, 5'-GGCAGC-CAGCTCAGCCATG-3' (26). The relative -fold change in the mRNA level was quantified using the 2- $\Delta\Delta C_t$  mathematical model (27).

**Animal Treatments**—Anti-Fx1A was produced and characterized as described in previous studies (7, 12). The antibody was obtained by immunizing sheep with tubular epithelial cell antigen (anti-Fx1A) from rat kidney cortex (kindly provided by Dr. Sudhir V. Shah). This antibody induces a complement-dependent injury, with granular deposits of sheep IgG and rat C3 in a generalized diffuse pattern along the capillary walls by immunofluorescence. PHN was induced in male Sprague-Dawley rats by a single intravenous injection of anti-Fx1A at a dose of 3 mg/100 g of body weight. *CYP2B1* was inhibited by two different inhibitors. Piperine, which inhibits *CYP2B1* by forming an inhibitory complex with the enzyme, was administered at a dose of 85 mg/kg of body weight by an intraperitoneal injection 16 h prior to anti-Fx1A treatment and then once a day (28). Cimetidine was injected intraperitoneally at a dose of 120 mg/kg of body weight 1 h prior to anti-Fx1A injection and then twice a day as described previously (29). The animals were killed on the fourth day with the onset of significant proteinuria.

**Immunofluorescence**—In the animal study, immunofluorescence was performed to test the binding force of anti-Fx1A using FITC-conjugated rabbit anti-sheep IgG (Zymed Laboratories Inc., San Francisco, CA). The MAC formation was detected using rabbit anti-C5b-9 antibody as the primary antibody (Calbiochem). In the measurement of nephrin, rabbit anti-mouse nephrin antibody (kindly provided by Dr. Lawrence Holzman) was used as the primary antibody. Fluorescence density was measured by outlining the perimeter of six to eight glomeruli and reading the luminosity from the Histogram command in the Image menu in Adobe Photoshop. For the *in vitro* study, GECs (with or without transfection) were washed with Dulbecco's PBS and incubated with anti-Fx1A (4 mg/ml) for 40 min at 22 °C. Cells were then washed, and fresh medium containing 5% FHS or HIS was added and incubated at 37 °C for 1 h. After incubation, cells were washed with PBS and fixed in 4% paraformaldehyde for 10 min at room temperature, followed by permeabilization with 0.1% Triton X-100 for 5 min also at room temperature. The cells were washed with PBS and labeled with Alexa Fluor 488-phalloidin (Invitrogen) and counterstained with DAPI (Invitrogen) as recommended by the manufacturer. In some experiments, cells were stained with ethidium homodimer-1 (Invitrogen) for 20 min as suggested by the manufacturer. Stained cells were then fixed, permeabilized, and labeled with Alexa Fluor 488-phalloidin. Fluorescence was observed using a Nikon Eclipse TS100F inverted microscope equipped with a DAPI, FITC, or Cy3 filter at ×400 magnification. Images were captured by a Nikon DS cooled camera and analyzed with NIS Elements Basic Research 3.0 software.

**Immunohistochemistry**—Kidney cortical sections were fixed in 10% buffered formalin for 6 h and embedded in paraffin. After deparaffinization and antigen retrieval, the sections were immunolabeled and visualized according to an avidin-

biotin complex method (30). The primary antibody for detection of the lipid peroxidation adduct malondialdehyde was rabbit anti-malondialdehyde polyclonal antibody (kindly provided by Dr. Dennis Peterson).

**Bleomycin-detectable Iron Assay**—Iron capable of catalyzing free radical reactions was measured by the bleomycin-detectable iron assay as described by Gutteridge *et al.* (31, 32) and as detailed in our previous studies (19, 33–35).

**Ultrastructural Localization of H<sub>2</sub>O<sub>2</sub>**—The principle of this method is that cerous iron combines with H<sub>2</sub>O<sub>2</sub> generated by the cell, which results in a precipitate with properties suitable for ultrastructural histochemistry (36). Localization of H<sub>2</sub>O<sub>2</sub> generation was performed following the procedure of Neale *et al.* (37) and as described in our previous study (28). In brief, following anti-Fx1A treatment, the left kidney was perfused at 37 °C by retrograde aortic perfusion with 4 ml of each of the following solutions: (i) PBS; (ii) 20 mmol/liter Tris maleate buffer (pH 7.2) containing 7% sucrose (TMS buffer); (iii) TMS buffer containing 1 mmol/liter aminotriazole; (iv) TMS buffer containing 10 mmol/liter aminotriazole, 1 mmol/liter cerium chloride heptahydrate, and 2.56 mmol/liter β-NADPH; and (v) TMS buffer, followed by 10 mmol/liter 2.5% glutaraldehyde as a fixative. Pieces of the kidney were fixed further for 2 h in glutaraldehyde and embedded in Epon. Sections from the tissue block were routinely stained with 4% aqueous uranyl acetate and alkaline lead and examined under a Leo 906 electron microscope.

**Western Blot Analysis**—For detection of CYP2B1 in the rat kidney, the microsome fraction of glomeruli was isolated as described in our previous study (29). In the nephrin study, a cellular fraction of kidney cortex was obtained by homogenizing the kidney cortex in 0.05 mol/liter Tris-HCl and 0.25 mol/liter sucrose (pH 7.4), followed by centrifugation at 10,000 × *g* for 20 min. In the *in vitro* study, cell lysate was collected by lysis of cultured cells in a radioimmune precipitation assay buffer that contained a protease inhibitor mixture (Sigma). Samples were subjected to SDS-PAGE in 1-mm slab gels. The separated forms were transferred from the gel to a nitrocellulose sheet using a Mini Trans-Blot electroblotting unit (Bio-Rad). Subsequent to primary and secondary antibody (peroxidase-labeled) treatment, the blots were visualized by the enhanced chemiluminescence method (38) and quantified by densitometry (UnScan-It Gel Version 6.1, Silk Scientific, Orem, UT). The anti-CYP2B1 antibody was purchased from Millipore (Temecula, CA); the rabbit anti-rat gelsolin polyclonal antibody was purchased from Abcam (Cambridge, MA); and the anti-mouse actin antibody was purchased from Millipore.

**Additional Assay**—Urinary protein was determined by the Bradford method with bovine serum albumin as the standard.

**Statistical Analysis**—Values are expressed as the mean ± S.E. Statistical analysis was performed using an unpaired *t* test (for two groups only) and analysis of variance (for more than two groups). Statistical significance was considered at *p* < 0.05.

## RESULTS

**Overexpression of CYP2B1 in GECs Exacerbates Complement-induced H<sub>2</sub>O<sub>2</sub> Generation and Cytotoxicity**—Incubation of GECs overexpressing CYP2B1 with anti-Fx1A and fresh human serum (source of complement) resulted in a time-dependent increase in complement-related H<sub>2</sub>O<sub>2</sub> generation. It also induced cytotoxicity as measured by LDH release compared with cells infected with a negative (empty) adenovirus (Fig. 1, *A* and *B*). These data suggest that the changes seen are gene-specific and caused by CYP2B1 overexpression. CYP2B1 gene silencing resulted in a significant decrease in CYP2B1 mRNA and protein by ~65% (21) and prevented the increase in complement-mediated H<sub>2</sub>O<sub>2</sub> generation and cytotoxicity (LDH release) compared with scrambled or negative siRNA-transfected cells (Fig. 1, *C* and *D*).

**Complement-mediated Loss of CYP2B1 Is a Post-translational Event**—The breakdown of the CYP2B1 protein is essential for the generation of ROS and sublytic injury. Treatment of the infected GECs with FHS for 1 h resulted in a significant decrease in CYP2B1 protein (Fig. 2*A*). However, CYP2B1 mRNA levels measured at the same time were not significantly different compared with cells treated with HIS (Fig. 2*B*). These results suggest that complement-mediated loss of CYP2B1 protein is a translational or post-translational event.

**CYP2B1 Overexpression in GECs Enhances Complement-mediated Membrane Permeability and Disruption of the Actin Microfilaments**—Ethidium homodimer enters cells and stains the nucleus with bright red fluorescence when the plasma membrane is permeabilized. Hence, it is a useful marker of C5b-9-induced permeabilization of the cell membrane (8). Cells were also stained by calcein, which is taken up by live cells only and emits green fluorescence. The extent of complement-mediated injury was quantitated by counting the number of cells with stained nuclei. Treatment of GECs infected with a negative adenovirus with anti-Fx1A increased cell membrane permeability as demonstrated by the increase in red fluorescence in cells in the presence of FHS, but not HIS (Fig. 3, *A* and *B*). This response was exacerbated by ectopic overexpression of the CYP2B1 (Fig. 3, *C* and *D*). Knockdown of CYP2B1 expression in the cells overexpressing CYP2B1 significantly attenuated cell membrane permeability (Fig. 3*F*), whereas scrambled siRNA did not change the permeability (Fig. 3*E*). Cells overexpressing CYP2B1 exposed to anti-Fx1A and FHS showed marked disruption of the actin microfilaments and loss of lamellipodia (Fig. 4*B*) compared with cells infected with negative virus and treated with anti-Fx1A and HIS (Fig. 4*A*). Knockdown of CYP2B1 expression preserved the actin cytoskeleton and lamellipodia (Fig. 4*D*) after treatment with FHS as opposed to a scrambled siRNA (Fig. 4*C*).

**Complement-mediated Membrane Permeabilization and Disruption of the Actin Cytoskeleton Are Reversible Events**—GECs that overexpressed CYP2B1 were treated with FHS as a source of complement for 1 h. Following incubation, the medium was changed to fresh growth medium for 18 h, and the cells were stained with calcein/ethidium homodimer or

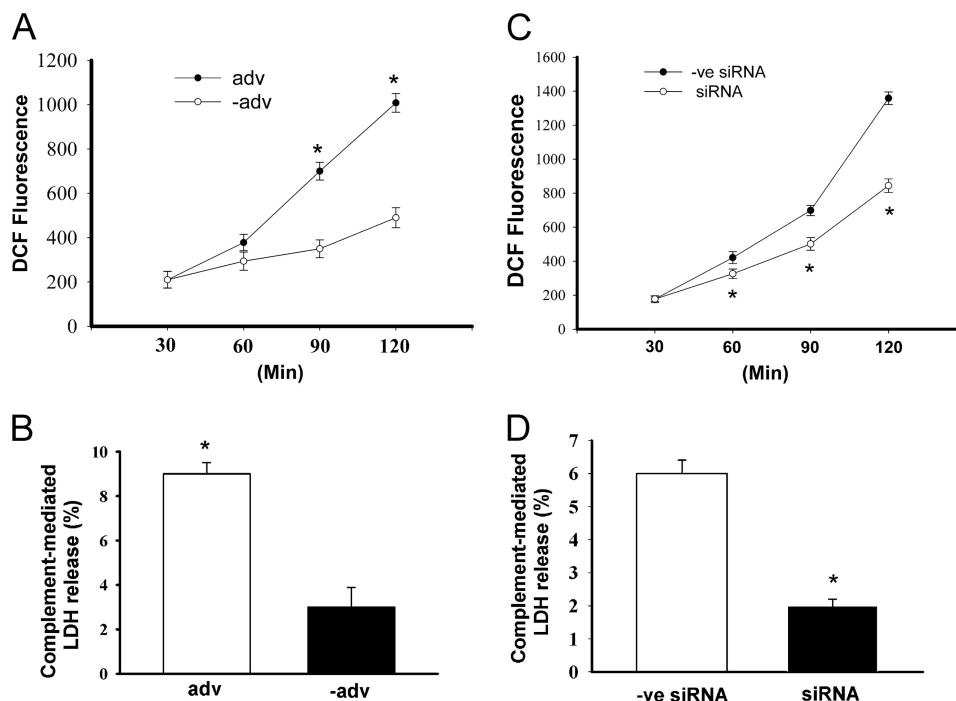


FIGURE 1. **Effect of up- and down-regulation of CYP2B1 expression on anti-Fx1A-induced H<sub>2</sub>O<sub>2</sub> generation and cytotoxicity in GECs.** A and B, GECs were infected with the CYP2B1-expressing adenovirus (*adv*) or an empty adenovirus (*-adv*), followed by treatment with 4 mg/ml anti-Fx1A, and then incubated with FHS or HIS (5%) for 1 h. Generation of H<sub>2</sub>O<sub>2</sub> was measured between 0.5 to 2 h after treatment by the oxidant-sensitive fluorescent dye dichlorodihydrofluorescein diacetate (DCF) (A). Data at each time point in both the adenovirus and empty adenovirus groups represent net complement-mediated generation of H<sub>2</sub>O<sub>2</sub> by FHS minus the endogenous generation of H<sub>2</sub>O<sub>2</sub> by HIS. Cytotoxicity was determined by LDH release (B). Data in both the adenovirus and empty adenovirus groups represent net complement-mediated percentage of LDH release by FHS minus the endogenous LDH release by HIS. C and D, the CYP2B1 was silenced in GECs infected with CYP2B1 adenovirus for 48 h. GECs were then treated with anti-Fx1A followed by FHS or HIS. A negative siRNA (*-ve siRNA*) group was included to reflect the specificity of our silencing effect. H<sub>2</sub>O<sub>2</sub> generation (C) and cytotoxicity (D) were measured as described. Values are means ± S.E. (n = 3). \*, p < 0.05 compared with the empty adenovirus (C) or negative siRNA (D).

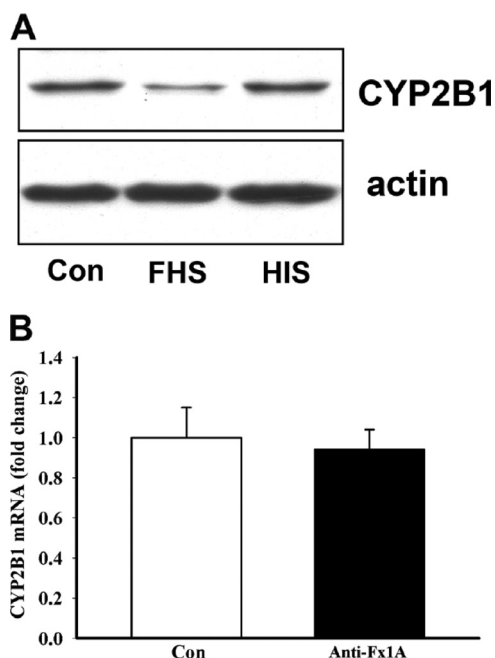
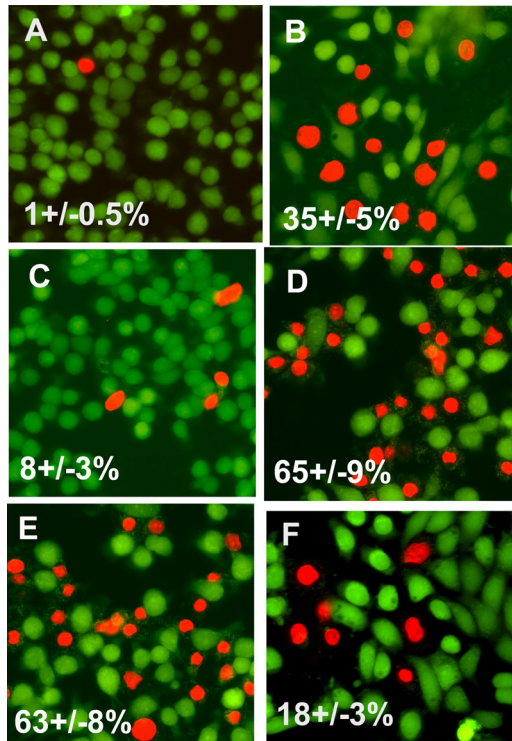


FIGURE 2. **Effect of anti-Fx1A on CYP2B1 protein levels and mRNA expression in GECs.** GECs were infected with CYP2B1 adenovirus, followed by treatment with anti-Fx1A (4 mg/ml) for 40 min at 22 °C, and incubated with FHS or HIS. A serum-free sample was used as a control. A, protein levels of CYP2B1 were determined by Western blotting. The blots are representatives of three independent experiments. B, CYP2B1 mRNA levels were determined by real-time RT-PCR. Values are means ± S.E. \*, p < 0.05 compared with the control (Con).

ethidium followed by phalloidin. As noted, the cells recovered from membrane permeabilization (Fig. 5, A and B) and cytoskeletal disorganization (Fig. 5, C and D) following removal of FHS. Cells with positive ethidium staining (Fig. 5C) exhibited collapse of the actin cytoskeleton compared with unstained cells (Fig. 5D). These data indicate the reversible and sublethal nature of complement-mediated injury and concur with the findings described by Salant and co-workers (8).

**Complement-mediated Disorganization of Actin Filaments Is Associated with Reduced Expression of Gelsolin**—Gelsolin is of fundamental importance in maintaining an organized actin cytoskeleton (39), and changes in this protein could account for the altered actin cytoskeletal reorganization as described above. GECs overexpressing CYP2B1 and transfected with scrambled siRNA were treated with either FHS or HIS for 1 h. Complement-mediated injury resulted in a significant decrease in the gelsolin protein. CYP2B1 gene silencing resulted in preservation of the gelsolin protein compared with GECs treated with scrambled siRNA (Fig. 6, A and B). Gelsolin mRNA was not down-regulated (Fig. 6C), suggesting that post-transcriptional factors determine the low gelsolin levels.

**Glomerular Immunofluorescence, Catalytic Iron, and Lipid Peroxidation**—Rats injected with sheep anti-Fx1A showed granular immune deposits of IgG in the glomeruli 1 h following injection, with increasing intensity of immune fluorescence by day 4 (Fig. 7A). Glomerular C5b-9 was detectable as early as 1 h, with deposits reaching maximum levels on day 4 (Fig. 7B). The bleomycin-detectable iron content was mark-



**FIGURE 3. Effects of overexpression or knockdown of CYP2B1 on complement-induced membrane permeabilization in cultured GECs.** Negative (A and B) or CYP2B1 (C and D) adenovirus-infected GECs were incubated with anti-Fx1A followed by HIS (A and C) or FHS (B and D) and stained with calcein and ethidium homodimer as described under "Experimental Procedures." In another set of experiments, CYP2B1-infected cells were treated with anti-Fx1A and FHS in the presence of scrambled (E) or CYP2B1-specific (F) siRNA. Fluorescence was detected as described under "Experimental Procedures." Images are representative of three independent experiments. The extent of membrane permeabilization (red staining) is expressed as a percentage of total cell numbers.

edly elevated in the glomeruli as early as 6 h following the injection of anti-Fx1A, with a tendency to increase at 1 h, and continued to remain elevated throughout the study (Fig. 7D). Immunohistochemistry demonstrated positive staining of malondialdehyde-modified proteins in the glomeruli and tubules as early as 1 h, with continual deposits throughout the course of study (Fig. 7C). The generation of malondialdehyde adducts occurred simultaneously with the formation of the MAC.

**Effect of CYP Inhibitors on PHN-induced Proteinuria**—A single intravenous injection of anti-Fx1A resulted in the onset of proteinuria on day 3, with a significant increase on day 4 (Fig. 8). Treatment with the CYP inhibitors piperine and cimetidine provided significant protection against anti-Fx1A-induced proteinuria (Fig. 8). Renal function as measured by blood urea nitrogen and serum creatinine was similar in all groups (data not shown).

**Mechanism by Which CYP2B1 Mediates Glomerular Injury in Vivo**—Utilizing an *in vivo* ultrastructural cerium histochemistry technique for H<sub>2</sub>O<sub>2</sub> localization, we demonstrated the presence of a electron-dense granular precipitate (cerium-H<sub>2</sub>O<sub>2</sub> complex) diffusely distributed throughout the major portion of the glomerular basement membrane on the fourth day following anti-Fx1A injection (Fig. 9A). These cerium-H<sub>2</sub>O<sub>2</sub> reaction products were significantly attenuated in the

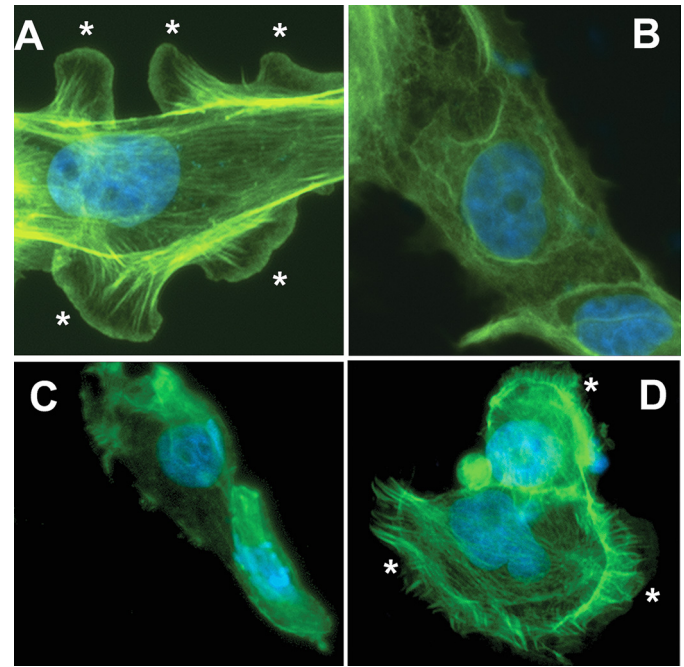


**FIGURE 4. Effects of overexpression or knockdown of CYP2B1 on organization of the actin cytoskeleton and lamellipodial formation in cultured GECs.** GECs were infected with the CYP2B1-expressing adenovirus (B–D) and treated with anti-Fx1A and FHS (B–D) in the presence of scrambled (C) or CYP2B1-specific (D) siRNA. A, cells infected with a negative virus, followed by incubation with anti-Fx1A and HIS. After treatment, cells were fixed, permeabilized, and stained with phalloidin and DAPI as described under "Experimental Procedures." Fluorescence was detected by microscopy, and images are representative of three independent experiments. The asterisks indicate lamellipodia.

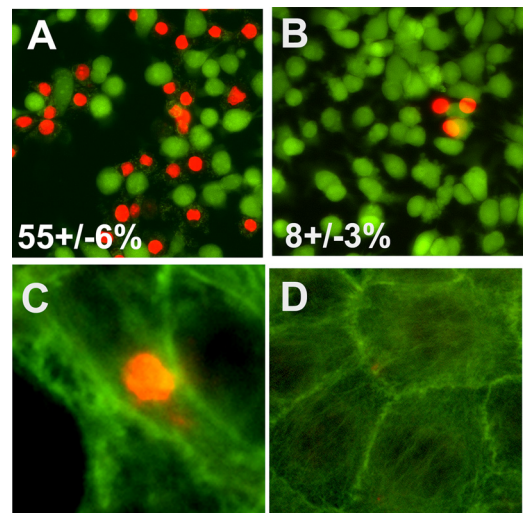


**FIGURE 5. Complement-induced membrane permeabilization and microfilament disorganization are reversible in cultured GECs.** Cultured GECs overexpressing CYP2B1 were treated with anti-Fx1A and FHS for 1 h (A and C) or were washed after this treatment and cultured for an additional 18 h in fresh culture medium (B and D). Cells were stained either with calcein/ethidium homodimer (A and B) or with ethidium homodimer followed by phalloidin (C and D). The percentage of red staining (membrane-permeabilized cells) was calculated. Images are representative of three independent experiments.

anti-Fx1A-injected rats treated with cimetidine (Fig. 9A). The glomerular immunostaining for the malondialdehyde adducts was markedly reduced following pretreatment of the PHN rats with cimetidine (Fig. 9B). The formation of the immune

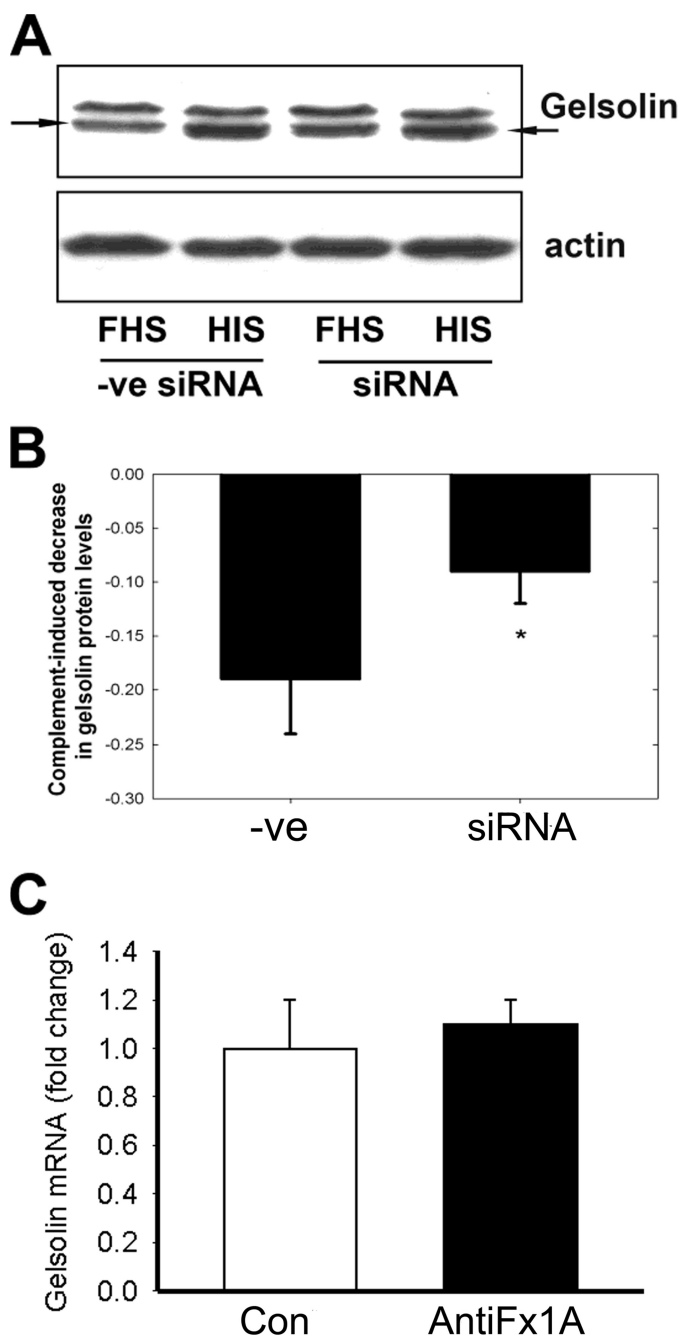


**FIGURE 6. Effect of CYP2B1 siRNA on anti-Fx1A-induced gelsolin protein levels and effect of anti-Fx1A on gelsolin mRNA expression in GECs.** The CYP2B1 was silenced in GECs infected with CYP2B1 adenovirus for 48 h. GECs were then treated with 4 mg/ml anti-Fx1A, followed by incubation with FHS or HIS. A negative siRNA (–ve siRNA) group was included to reflect the specificity of our silencing effect. *A*, the protein levels of gelsolin were determined by Western blotting. The blots are representative of three independent experiments. *B*, densitometry analysis of the Western blot result with gelsolin. The values represent net complement-mediated gelsolin protein decrease resulting from the loss of gelsolin protein by FHS minus the endogenous loss of gelsolin by HIS. Values are means ± S.E. ( $n = 3$ ). \*,  $p < 0.05$  compared with the negative siRNA group. *C*, GECs were infected with CYP2B1 adenovirus, followed by treatment with anti-Fx1A (4 mg/ml) for 40 min at 22 °C, and incubated with FHS. A serum-free sample was used as a control. Gelsolin mRNA levels were determined by real-time RT-PCR. Values are means ± S.E. \*,  $p < 0.05$  compared with the control (Con).

deposits and MAC was not affected by pretreatment with cimetidine (Fig. 9C). We next examined the effect of cimetidine on the bleomycin-detectable iron content in the glomeruli of

the anti-Fx1A-treated rats. Cimetidine significantly prevented an increase in catalytic iron content in the glomeruli of the PHN rats (Fig. 9D). The CYP2B1 content was markedly decreased in the anti-Fx1A-treated rats as indicated by Western blot analysis. Cimetidine prevented the loss of CYP2B1 content in the glomeruli of these animals (Fig. 9E).

**Effect of Cimetidine on Nephrin Distribution**—Nephrin is the major functional component of the glomerular filtration barrier. We therefore examined the distribution of nephrin at the onset of proteinuria and the effect of cimetidine in the anti-Fx1A-treated rats. Immunofluorescence staining of nephrin showed a linear pattern of nephrin distribution in normal glomeruli, and this normal distribution changed to a more granular pattern in the glomeruli of the anti-Fx1A-treated rats (Fig. 10A). Quantitative analysis showed a significant decrease in the fluorescence density in the PHN glomeruli (Fig. 10B). Cimetidine preserved the normal distribution of the nephrin and prevented a decrease in the fluorescence density (Fig. 10, A and B). Western blot analysis also demonstrated a significant decrease in nephrin content on day 3 of anti-Fx1A injection and further reduction on day 4 (Fig. 10C). The loss of nephrin was prevented by the administration of cimetidine (Fig. 10D).

**DISCUSSION**

In PHN, complement activation and localization of the MAC in subepithelial deposits result in sublytic damage to the GECs, followed by development of proteinuria 3–4 days after the injection of anti-Fx1A (40, 41). Several cellular and molecular mechanisms, including oxidants and iron (7, 12–13, 37, 42) with alterations in the cytoskeleton (3, 6), have been implicated in proteinuria.

The importance of the endoplasmic reticulum in complement-mediated injury to the GECs has been suggested (43). CYP enzymes are present at high concentrations in the endoplasmic reticulum and can be crucial in cell signaling and injury (44, 45). We conducted *in vitro* and *in vivo* studies to delineate the potential importance of a specific CYP in an immune-mediated model of glomerulonephritis. CYP monooxygenases catalyze oxidation of a variety of both endogenous and exogenous compounds, which leads to generation of superoxide anion, H<sub>2</sub>O<sub>2</sub>, and hydroxyl radical (46–48). In our studies, incubation of GECs overexpressing CYP2B1 with anti-Fx1A resulted in a significant increase in ROS generation and cytotoxicity. Silencing of CYP2B1 markedly reduced ROS generation and cytotoxicity. These results confirm that the changes in ROS generation and cytotoxicity are CYP2B1-dependent.

The cytoskeleton is critical for maintenance of podocyte foot processes and serves as a scaffold for transmitting signals from the extracellular environment and neighboring podocytes (6). Podocyte effacement and condensation of the foot process cytoskeleton are characteristic findings during antibody-dependent complement-mediated GEC injury in PHN (3). The actin cytoskeleton that supports the normal foot process architecture is one of the major cytoskeletal components (49). In our study, treatment of CYP2B1-overexpressing cells with anti-Fx1A and complement led to a significant increase

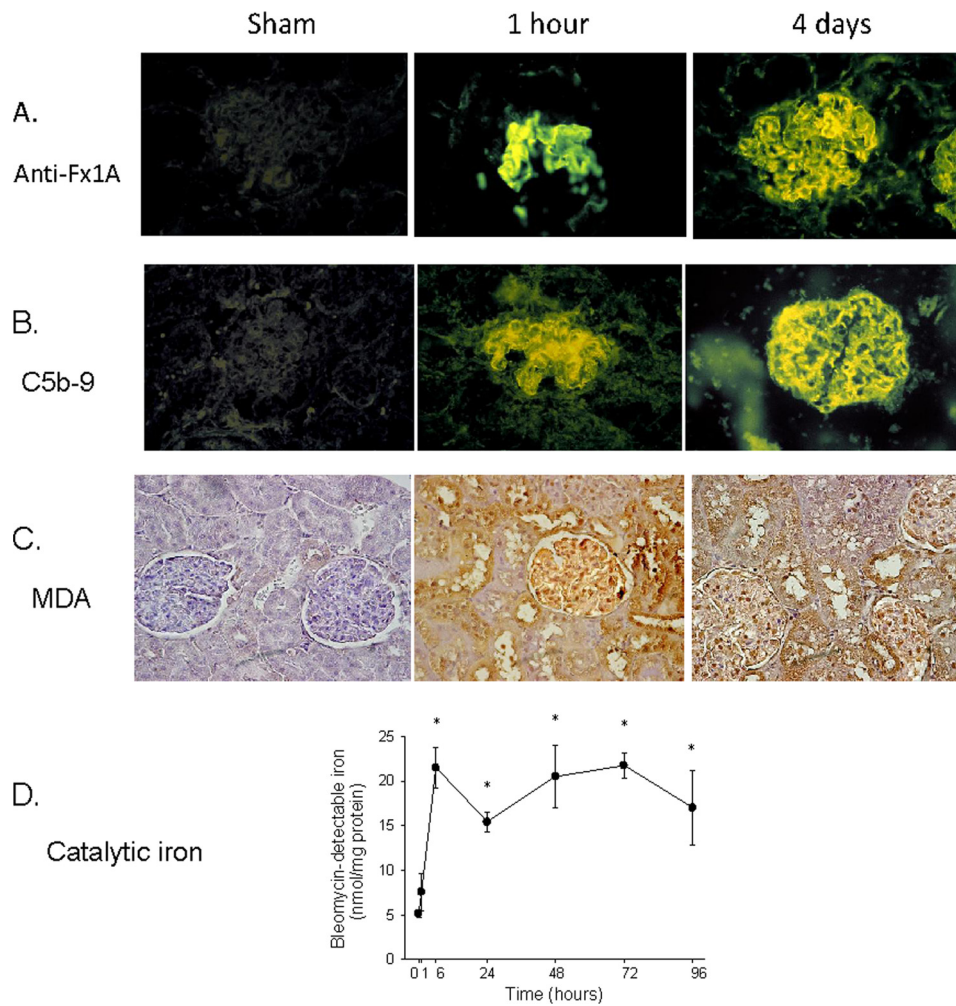


**FIGURE 7. Time courses of anti-Fx1A and C5b-9 depositions, lipid peroxidation, and catalytic iron release.** Rat glomeruli showed immune deposits of anti-Fx1A (A) and C5b-9 (B) 1 h following anti-Fx1A injection, with increasing intensity of immunofluorescence by the fourth day. C, immunostaining of malondialdehyde (MDA; a measurement for lipid peroxidation) demonstrated strong positive staining in the glomeruli and tubules as early as 1 h and on the fourth day. D, bleomycin-detectable iron (a measurement for catalytic iron) significantly increased at 6 h following anti-Fx1A treatment and throughout the course of the experiment. Values are means  $\pm$  S.E. ( $n = 5$ ).

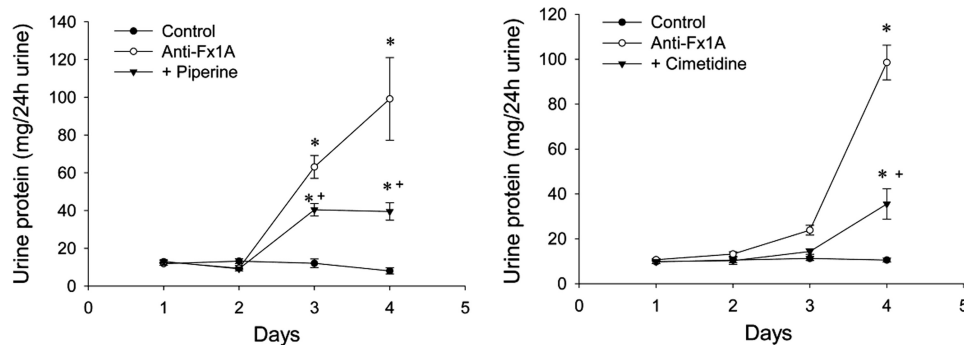


**FIGURE 8. Effect of the CYP inhibitors piperine and cimetidine on proteinuria (milligrams of urine/24 h) in rats treated with anti-Fx1A.** A single intravenous injection of anti-Fx1A resulted in the onset of proteinuria as early as day 3, with a significant increase on day 4. Treatment with piperine and cimetidine significantly reduced anti-Fx1A-induced proteinuria on days 3 and 4. Values are means  $\pm$  S.E. ( $n = 8$ ). \*,  $p < 0.05$  compared with the control; +,  $p < 0.05$  compared with anti-Fx1A.

in cell membrane permeability, ROS generation, and cytotoxicity accompanied by condensation of the actin cytoskeletal filaments to the base of the involved cell and loss of lamellipodia compared with control cells infected with negative virus and subjected to the same treatment. These results indicate that overexpression of *CYP2B1* exacerbates the cell injury. Moreover, *CYP2B1* gene

silencing attenuated cell membrane permeability, ROS generation, cytotoxicity, disruption of the actin cytoskeleton, and loss of lamellipodia induced by complement-mediated injury. We also showed that the increase in complement-mediated cell permeability and collapse of the actin cytoskeleton are sublytic and reversible.

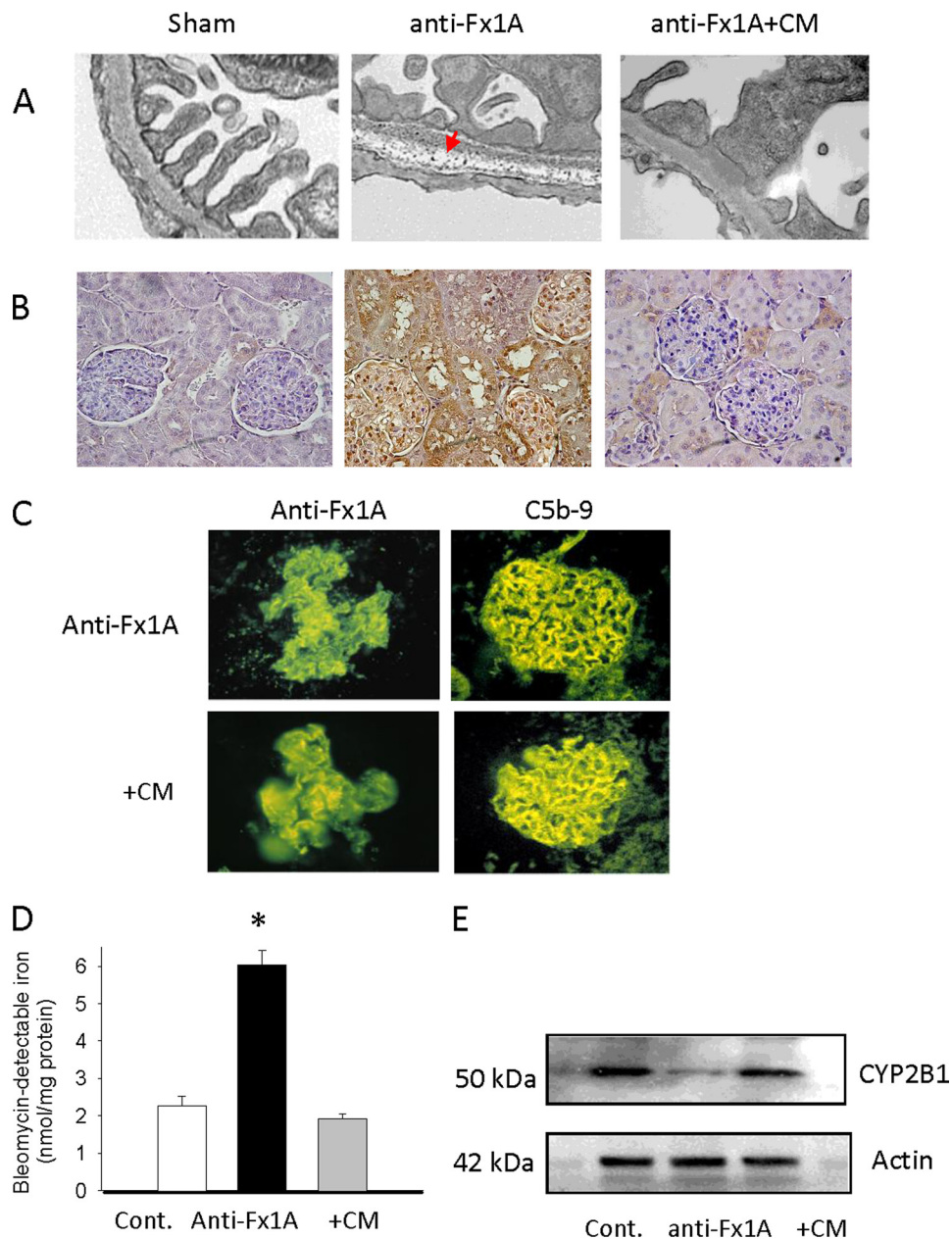


**FIGURE 9. Effects of CYP inhibitor on H<sub>2</sub>O<sub>2</sub> generation, lipid peroxidation, anti-Fx1A and C5b-9 deposition, catalytic iron formation, and CYP2B1 protein.** *A*, localization of H<sub>2</sub>O<sub>2</sub> by a histochemical cerium-H<sub>2</sub>O<sub>2</sub> precipitation method. Granular electron-dense cerium precipitation was predominant in the glomerular basement membrane in rat kidney on day 4 following anti-Fx1A injection (*middle panel, arrow*). This was significantly attenuated in rats treated with the CYP inhibitor cimetidine (CM). Control animals did not show any reaction product. *B*, immunohistochemistry staining of malondialdehyde (a measurement of lipid peroxidation) was significantly increased in anti-Fx1A-treated rats compared with control rats. Administration of the CYP inhibitor cimetidine markedly decreased the intensity of malondialdehyde staining in kidneys of anti-Fx1A-treated rats on day 4. *C*, immunofluorescence staining showed that cimetidine treatment did not alter the deposits of anti-Fx1A and C5b-9 compared with anti-Fx1A treatment alone. *D*, administration of cimetidine significantly reduced the catalytic iron content in kidneys of anti-Fx1A-treated rats. Values are means  $\pm$  S.E. ( $n = 5$ ). \*,  $p < 0.05$  compared with the control (*Cont.*). *E*, Western blot analysis of CYP2B1 protein levels in the glomeruli of rats injected with anti-Fx1A with or without administration of the CYP inhibitor cimetidine. The blots shown are representative of results from 5–10 animals per experimental group on day 4 following anti-Fx1A injection. CYP2B1 content was markedly decreased in the glomeruli of rats treated with anti-Fx1A, and this was significantly attenuated by administration of cimetidine.

Cytoskeletal rearrangement occurs in a variety of cellular processes and involves a wide spectrum of proteins. Among these, gelsolin is a highly conserved superfamily of multifunctional actin-binding proteins that have been implicated in the dynamic rearrangement of the cytoskeletal architecture (11). Gelsolin is expressed in normal kidneys and has been localized to the podocyte (9, 10). In our study, we demonstrated that CYP2B1-mediated comple-

ment injury resulted in disorganization/loss of the actin cytoskeleton accompanied by loss of gelsolin protein. Silencing of CYP2B1 resulted in maintenance of the actin cytoskeleton and preservation of gelsolin. This could imply that gelsolin is crucial in maintaining cytoskeletal integrity.

In PHN, the development of proteinuria is related to formation of the MAC and generation of ROS by glomerular cells (42, 50). However, the precise site and source involved in

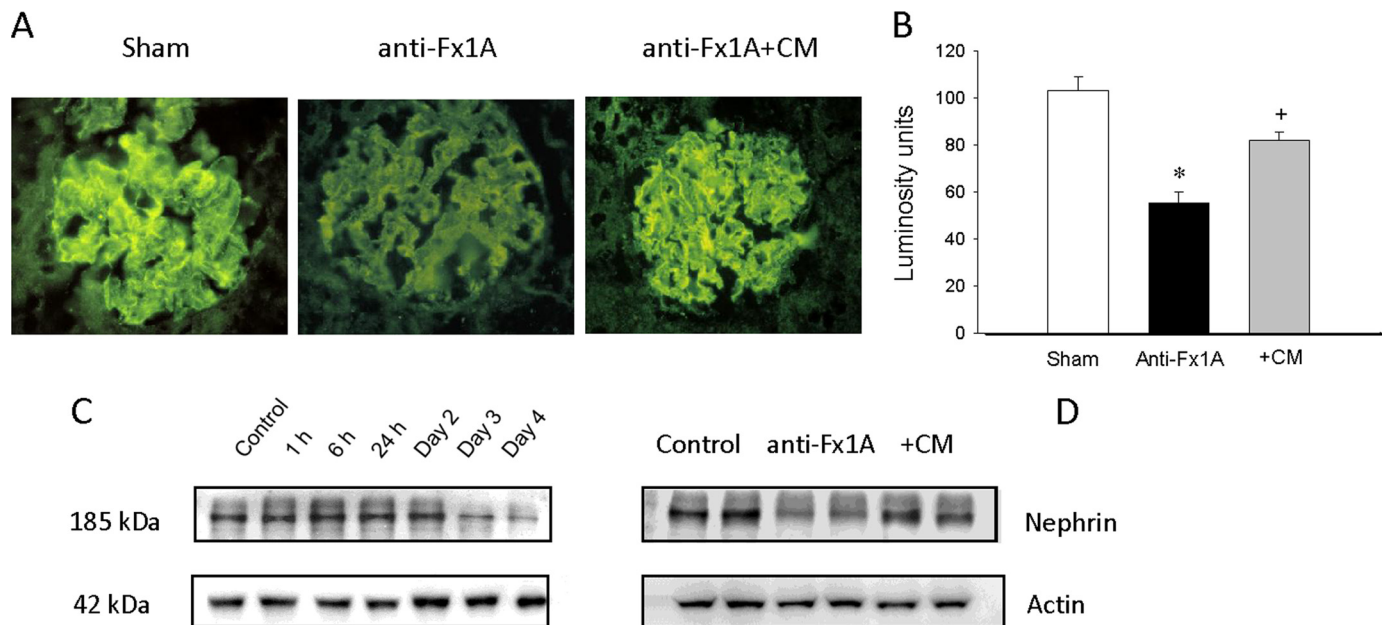


**FIGURE 10. Changes of nephrin in PHN.** *A* and *B*, the changes in nephrin distribution were measured by immunofluorescence. The linear pattern of nephrin distribution was altered in the glomeruli of anti-Fx1A-treated rats on day 4 following anti-Fx1A treatment. The CYP inhibitor cimetidine (CM) preserved the normal distribution of nephrin (*A*). Fluorescence density was measured by outlining the perimeter of six to eight glomeruli and reading the luminescence from the Histogram command in the Image menu of Adobe Photoshop (*B*). All exposure settings were kept constant for each group of kidneys. The fluorescence density in the glomeruli of anti-Fx1A-treated rats was significantly decreased compared with controls. Values are means  $\pm$  S.E. ( $n = 6-8$ ). \*,  $p < 0.05$  versus the control; +,  $p < 0.05$  versus anti-Fx1A-treated rats. *C* and *D*, changes in nephrin protein levels were also measured by Western blot analysis. Nephrin was significantly reduced on day 3 following anti-Fx1A injection with further reduction on day 4 (*C*). This decrease in nephrin was significantly prevented by administration of cimetidine on day 4 following anti-Fx1A treatment (*D*). The blots shown are representative of results from 5–10 animals per experimental group.

ROS generation are currently not known. Using an ultrastructural cerium histochemistry technique, we demonstrated electron-dense precipitates, which involve a major portion of the glomerular basement membrane, in anti-Fx1A-treated animals with the onset of proteinuria. There was little or no cerium- $H_2O_2$  reaction product in the PHN rats treated with the CYP2B1 inhibitor cimetidine. Utilizing a monoclonal antibody for malondialdehyde as a marker of lipid peroxidation, we demonstrated a marked increase in the malondialdehyde adducts in the glomeruli with the onset of proteinuria in the PHN rats. ROS can also cause structural changes in the glomerular basement membrane by lipid peroxidation, which leads to the generation of highly reactive compounds such as malondialdehyde (51). We have shown that the CYP heme moiety may serve as a significant source of iron capable of catalyzing free radical reactions (29). The bleomycin-detectable iron content was markedly elevated and was associated with a significant decrease in CYP2B1 protein content in the glomeruli of the anti-Fx1A-treated rats. Cimetidine not only markedly decreased the  $H_2O_2$  generation, as described above, but also prevented an increase in bleomycin-detectable iron, loss of CYP2B1 protein in the glomeruli, and accumulation of malondialdehyde adducts, with significant protection against anti-Fx1A-induced proteinuria. Our *in vitro* data further indicate that the loss of CYP2B1 protein occurs as a translational or post-translational event and is not the effect of transcriptional regulation.

A characteristic feature of PHN is podocyte injury, resulting in proteinuria. Nephrin is the major functional component of the glomerular filtration barrier (52). Nephrin mRNA levels and protein content decline progressively in the glomeruli of rats with PHN and established proteinuria (53). In PHN, there is a redistri-

bution and loss of nephrin from the glomerular podocytes that occur with or prior to the onset of proteinuria (52). Our studies indicate a change in the distribution of nephrin in the glomeruli (by immunofluorescence) with the onset of proteinuria. This is associated with a marked reduction of nephrin. Treatment with cimetidine preserved the normal pattern of distribution of nephrin in the glomeruli of the PHN rats and prevented the reduction of nephrin. The changes in nephrin content were also assessed by Western blot analysis. The blots demonstrated a significant decrease in nephrin content on day 3 of anti-Fx1A injection and a further reduction on day 4. The loss of nephrin was prevented following administration of cimetidine.

Together, these results demonstrate that CYP2B1 serves as a major site for ROS generation, is a significant source of catalytic iron, and plays an important role in alterations in the cytoskeleton, all processes that have been implicated in proteinuria. These findings provide a basis for identifying corresponding CYP forms in human kidneys and investigating novel interactive pathways that would ultimately lead to potential therapeutic targets in the treatment of membranous nephropathy in humans.

*Acknowledgments*—We thank Drs. Lawrence Holzman and Dennis Peterson for providing antibodies used in this study and Cindy Reid (University of Arkansas for Medical Sciences) for technical editing of the manuscript.

## REFERENCES

- Beck, L. H., Jr., Bonegio, R. G., Lambeau, G., Beck, D. M., Powell, D. W., Cummins, T. D., Klein, J. B., and Salant, D. J. (2009) *N. Engl. J. Med.* **361**, 11–21

2. United States Renal Data System (2009) *Atlas of End-stage Renal Disease: Annual Data Report*, NIDDK, National Institutes of Health, Bethesda, MD
3. Salant, D. J., Quigg, R. J., and Cybulsky, A. V. (1989) *Kidney Int.* **35**, 976–984
4. Couser, W. (1993) *Kidney Int.* **44**, S19–S26
5. Cybulsky, A. V., Quigg, R. J., and Salant, D. J. (2005) *Am. J. Physiol. Renal Physiol.* **289**, F660–F671
6. Patrakka, J., and Tryggvason, K. (2009) *Nat. Rev. Nephrol.* **5**, 463–468
7. Shah, S. V. (1988) *Am. J. Physiol.* **254**, F337–F344
8. Topham, P. S., Haydar, S. A., Kuphal, R., Lightfoot, J. D., and Salant, D. J. (1999) *Kidney Int.* **55**, 1763–1775
9. Harvey, S. J., Jarad, G., Cunningham, J., Goldberg, S., Schermer, B., Harfe, B. D., McManus, M. T., Benzing, T., and Miner, J. H. (2008) *J. Am. Soc. Nephrol.* **19**, 2150–2158
10. Lueck, A., Brown, D., and Kwiatkowski, D. J. (1998) *J. Cell Sci.* **111**, 3633–3643
11. dos Remedios, C. G., Chhabra, D., Kekic, M., Dedova, I. V., Tsubakihara, M., Berry, D. A., and Nosworthy, N. J. (2003) *Physiol. Rev.* **83**, 433–473
12. Baliga, R., Baliga, M., and Shah, S. V. (1992) *Am. J. Physiol.* **263**, F56–F61
13. Baliga, R., Ueda, N., and Shah, S. V. (1996) *J. Am. Soc. Nephrol.* **7**, 1183–1188
14. Kuthan, H., Tsuji, H., Graf, H., and Ullrich, V. (1978) *FEBS Lett.* **91**, 343–345
15. Nordblom, G. D., and Coon, M. J. (1977) *Arch. Biochem. Biophys.* **180**, 343–347
16. Gutteridge, J. M. C. (1986) *FEBS Lett.* **201**, 291–295
17. Bysani, G. K., Kennedy, T. P., Ky, N., Rao, N. V., Blaze, C. A., and Hoidal, J. R. (1990) *J. Clin. Invest.* **86**, 1434–1441
18. Paller, M. S., and Jacob, H. S. (1994) *Proc. Natl. Acad. Sci. U.S.A.* **91**, 7002–7006
19. Baliga, R., Zhang, Z., Baliga, M., and Shah, S. V. (1996) *Kidney Int.* **49**, 362–369
20. Baliga, R., Zhang, Z., and Shah, S. V. (1996) *Kidney Int.* **50**, 1118–1124
21. Tian, N., Arany, I., Waxman, D. J., and Baliga, R. (2010) *Kidney Int.* **78**, 182–190
22. Liu, H., Baliga, M., Bigler, S. A., and Baliga, R. (2003) *Exp. Nephrol.* **94**, e17–e24
23. Tzanakakis, E. S., Waxman, D. J., Hansen, L. K., Rimmel, R. P., and Hu, W. S. (2002) *Cell Biol. Toxicol.* **18**, 13–27
24. Rosenkranz, A. R., Schmaldienst, S., Stuhlmeier, K. M., Chen, W., Knapp, W., and Zlabinger, G. J. (1992) *J. Immunol. Methods* **156**, 39–45
25. Quigg, R. J., Cybulsky, A. V., Jacobs, J. B., and Salant, D. J. (1988) *Kidney Int.* **34**, 43–52
26. Ni, X. G., Zhou, L., Wang, G. Q., Liu, S. M., Bai, X. F., Liu, F., Peppelenbosch, M. P., and Zhao, P. (2008) *Mol. Med.* **14**, 582–589
27. Livak, K. J., and Schmittgen, T. D. (2001) *Methods* **25**, 402–408
28. Liu, H., Bigler, S. A., Henegar, J. R., and Baliga, R. (2002) *Kidney Int.* **62**, 868–876
29. Liu, H., Shah, S. V., and Baliga, R. (2001) *Am. J. Physiol. Renal Physiol.* **280**, F88–F94
30. Hsu, S. M., Raine, L., and Fanger, H. (1981) *J. Histochem. Cytochem.* **29**, 577–580
31. Gutteridge, J. M., Rowley, D. A., and Halliwell, B. (1981) *Biochem. J.* **199**, 263–265
32. Gutteridge, J. M., Rowley, D. A., and Halliwell, B. (1982) *Biochem. J.* **206**, 605–609
33. Baliga, R., Zhang, Z., Baliga, M., Ueda, N., and Shah, S. V. (1998) *Kidney Int.* **54**, 1562–1569
34. Baliga, R., Zhang, Z., Baliga, M., Ueda, N., and Shah, S. V. (1998) *Kidney Int.* **53**, 394–401
35. Ueda, N., Baliga, R., and Shah, S. V. (1996) *Kidney Int.* **49**, 370–373
36. Briggs, R. T., Drath, D. B., Karnovsky, M. L., and Karnovsky, M. J. (1975) *J. Cell Biol.* **67**, 566–586
37. Neale, T. J., Ullrich, R., Ojha, P., Poczewski, H., Verhoeven, A. J., and Kerjaschki, D. (1993) *Proc. Natl. Acad. Sci. U.S.A.* **90**, 3645–3649
38. Bradd, S. J., and Dunn, M. J. (1993) *Methods Mol. Biol.* **19**, 211–218
39. Silacci, P., Mazzolai, L., Gauci, C., Stergiopoulos, N., Yin, H. L., and Hayoz, D. (2004) *Cell. Mol. Life Sci.* **61**, 2614–2623
40. Cybulsky, A. V., Renneke, H. G., Feintzeig, I. D., and Salant, D. J. (1986) *J. Clin. Invest.* **77**, 1096–1107
41. Johnson, R. J., Couser, W. G., Chi, E. Y., Adler, S., and Klebanoff, S. J. (1987) *J. Clin. Invest.* **79**, 1379–1387
42. Baliga, R., Ueda, N., and Shah, S. V. (1997) in *Current Nephrology* (Gonick, H., ed) pp. 135–151, Mosby-Year Book, Inc., Chicago
43. Cybulsky, A. V., Takano, T., Papillon, J., Khadir, A., Liu, J., and Peng, H. (2002) *J. Biol. Chem.* **277**, 41342–41351
44. Bondy, S. C., and Naderi, S. (1994) *Biochem. Pharmacol.* **48**, 155–159
45. Rashba-Step, J., and Cederbaum, A. I. (1994) *Mol. Pharmacol.* **45**, 150–157
46. Gonzalez, F. J. (1988) *Pharmacol. Rev.* **40**, 243–288
47. Kappus, H. (1993) *Handb. Exp. Pharmacol.* **105**, 145–154
48. Karuzina, I. I., and Archakov, A. I. (1994) *Free Radic. Biol. Med.* **16**, 73–97
49. Mundel, P., and Kriz, W. (1995) *Anat. Embryol.* **192**, 385–397
50. Couser, W. G., and Abrass, C. K. (1988) *Annu. Rev. Med.* **39**, 517–530
51. Neale, T. J., Ojha, P. P., Exner, M., Poczewski, H., Rüger, B., Witztum, J. L., Davis, P., and Kerjaschki, D. (1994) *J. Clin. Invest.* **94**, 1577–1584
52. Yuan, H., Takeuchi, E., Taylor, G. A., McLaughlin, M., Brown, D., and Salant, D. J. (2002) *J. Am. Soc. Nephrol.* **13**, 946–956
53. Benigni, A., Tomasoni, S., Gagliardini, E., Zoja, C., Grunkemeyer, J. A., Kalluri, R., and Remuzzi, G. (2001) *J. Am. Soc. Nephrol.* **12**, 941–948